(19) Europäisches Patentamt
European Patent Office
Office européen des brevets

(11) Publication number: 0 361 810 B1

(12) EUROPEAN PATENT SPECIFICATION

(45) Date of publication of patent specification: 14.12.94 Bulletin 94/50

(51) Int. Cl.[5]: G01N 27/42

(21) Application number: 89309683.4

(22) Date of filing: 22.09.89

(54) Pulsed coulometric detection.

(30) Priority: 26.09.88 US 249014

(43) Date of publication of application: 04.04.90 Bulletin 90/14

(45) Publication of the grant of the patent: 14.12.94 Bulletin 94/50

(84) Designated Contracting States: AT BE CH DE ES FR GB GR IT LI LU NL SE

(56) References cited:
EP-A- 0 242 530
CH-A- 659 327
FR-A- 2 551 548
FR-A- 2 583 879
ANALYTICAL CHEMISTRY vol. 45, no. 11, 11 September 1973, pages 1864 - 1868; YOSHINORI TAKATA: 'FLOW COULOMETRIC DETECTOR FOR LIQUID CHROMATOGRAPHY'

(56) References cited:
JOURNAL OF THE ELECTROCHEMICAL SOCIETY vol. 117, no. 12, 31 December 1970, pages 1500 - 1506; D. E. ICENHOWER: 'USE OF THE POTENTIAL-STEP METHOD TO MEASURE SURFACE OXIDES'
Analytica Chemical Acta, vol. 192, 1987, pages 205-218.

(73) Proprietor: IOWA STATE UNIVERSITY RESEARCH FOUNDATION, INC.
315 Beardshear Hall
Ames, Iowa 50011 (US)

(72) Inventor: Johnson, Dennis C.
Rural Route 4
Ames Iowa 50010 (US)
Inventor: Neuberger, Glen G.
6 Twain Court
Freehold New Jersey 07728 (US)

(74) Representative: Cross, Rupert Edward Blount et al
BOULT, WADE & TENNANT
27 Furnival Street
London EC4A 1PQ (GB)

EP 0 361 810 B1

Description

The United States Government has rights to the invention herein through the National Science Foundation, Contract CHE-8312032, with Iowa State University.

Intense interest has developed related to the direct electrochemical detection of aliphatic compounds based on electrocatalytic reactions at noble metal electrodes, chiefly Au and Pt. Electrochemical detection is a widely accepted means of detection in liquid and ion chromatrography. Electrochemical detectors operate by applying an electric potential to the working electrode in a flow-through cell. Such detectors typically employ a three-electrode cell including a working electrode, a reference electrode and a counter electrode. The methodology relies on use of multi-step potential waveforms which incorporate a detection operation along with the anodic cleaning and cathodic reactivation of the electrode surface. A typical potential waveform is shown in Fig. 1A. Anodic detection occurs at potential E_1 with current sampling during a 16.7-ms period at the end of period t_1. The potential then is stepped to E_2 (period t_2), for oxidative cleaning of the electrode surface, and subsequently to E_3 (period t_3) for reactivation by cathodic dissolution of the surface oxide formed at E_1 and/or E_2. Adsorption of analyte also can occur at E_3 and for long t_3 the concentration of analyte at the electrode surface is reestablished to the value of the bulk solution ($c^s = c^b$). The analytical application of this method, now known as Pulsed Amperometric Detection (PAD), has been demonstrated for alcohols, polyalcohols and carbohydrates (reducing and non-reducing) (1-6); amines and amino acids (primary and secondary) (7); aminoglycosides (8); and numerous sulfur compounds (except sulfate, sulfonic acids and sulfones) (9-11).

Recently, Pulsed Coulometric Detection (PCD) was described (12). The significant difference between PAD and PCD lies in the instrumental protocol related to measurement of the faradaic signal. In PAD, electrode current is averaged over a time period of 16.7 ms (i.e., 1/60 Hz^{-1}) whereas in PCD the amperometric response is electronically integrated over an integral number of sequential 16.7-ms periods (12). PCD inherently has a larger signal-to-noise ratio (S/N) because of the larger signal strength and because the integral of a 60-Hz correlated noise signal, a predominant form of noise in electronic instrumentation, remains at zero over the integration period.

One limitation of indirect PCD methods is that unless there is a significant interaction between the electrode and the background chemical(s), no result is attained. For example, reference (15) discloses an indirect method wherein an initial chemical adsorption reaction between a working electrode and hydrogen establishes an electrical current, which current is then attenuated by an adsorption reaction between the working electrode and a chemical analyte. In reference (15), it is understood that the working electrode may be platinum, but, for example, cannot be gold, since hydrogen atoms will not adsorb gold. Conversely, regardless of the working electrode composition, the pre-measurement phase electrode-chemical adsorption requirement precludes indirect measurements for those chemicals that do not adsorb to the working electrode. By contrast, the presently claimed direct method does not impose a chemical-electrode reaction as an absolute prerequisite to detection.

With the advent of more complex liquid chromatographic techniques which employ a variety of gradient elution methods, it is necessary to develop detectors which are capable of sustaining high values of sensitivity and detectability over the gradient period, and which also can reject automatically the accompanying variation in background signal. Detectors traditionally used for aliphatic compounds cannot be used in pH-gradient liquid chromatography (LC) because they are affected by changes in ionic strength. Photometric detection suffers because of an inherently low sensitivity for aliphatic compounds without extensive π -bonding and because of baseline drift which accompanies a change in the refractive index of the mobile phase. Refractive index detection is strongly affected by concentration gradients and the baseline shift observed for even small changes in mobile phase composition can overwhelm the analyte signal.

The methods of PAD (1-10) and PCD (12) were introduced for detection of numerous aliphatic organic compounds in conjunction with liquid chromatography (LC). However, the ability of either technique to resist even a slight pH change is strongly dependent on the detection potential and the electrode material selected. In fact, PAD at a Pt electrode in a flow-injection (FI) system has been suggested for the determination of pH changes in caustic media (13). Sensitivity of the baseline in PAD and PCD to changes in solution pH is greatest for amines and sulfur compounds at Au and Pt because the anodic detection reactions are catalyzed by simultaneous formation of surface oxide on the noble metal electrodes (7,9,10).

It is an object of the present invention to provide an improved pulsed coulometric detection method.

According to the present invention there is provided a liquid chromatographic pulsed coulometric detection method for direct detection of at least one analyte, comprising the following steps; applying an electrical potential waveform defining a potential sweep or potential step function to a working electrode in a flow-through cell, and electrochemically detecting analyte directly by integrating current over a cyclic detection portion of the total electric potential waveform.

The pulsed coulometric detection method according to the present invention is intended for use in electrochemical modes of detection which utilize anodic cleaning and cathodic reactivation of electrode surfaces in a liquid chromatographic environment.

In one preferred embodiment, the method comprises the steps of generating multi-step potential waveforms having cyclic potential changes where the cyclic waveforms have a first initial potential value (E1) for a first time period t_d so that the electrode surfaces exist in an oxide-free state, advancing (increasing) the potential value to a second, higher value ($E_{1'}$) for a time period t_s so as to cause the formation of surface oxide with concurrent electrocatalytic oxidative reaction of soluble and/or adsorbed analyte, and returning the potential value to said first value E_1 for a holding time period t_h, during which all oxide formed during the potential change to $E_{1'}$ is cathodically stripped from said electrode surfaces.

Other objects and features of the present invention will become apparent from the following detailed description when taken in conjunction with the accompanying drawings.

Brief Description of the Drawings

Fig. 1. Potential-time waveforms.
(A) PAD (B-D) PS-PCD.

Fig. 2. Current-potential response for thiourea at a Au RDE in 0.25 M NH_4NO_3 (pH 5.1).
Concentration (mM) : (A) 0.0, (B) 0.10,
(C) 0.30, (D) 0.50.

Figs. 3A & 3B
Current-potential and charge-potential response for thiourea at the Au RDE in 0.25 M NH_4NO_3 (pH 5.1).
Solutions: (A,C) blank, (B,D) 100 μM thiourea.
Curves: (A,B) current vs. potential (i-E),
(C,D) charge vs. potential (q-E).

Fig. 4.
Comparison of settling time and drift for PS-PCD and PAD in 0.25 M NH_4NO_3 (pH 5.1).
Waveforms: (PS-PCD) WF-3, (PAD) WF-1.

Fig. 5.
Comparison of detection peaks and baseline offset for PS-PCD and PAD in 0.25 M NH_4NO_3 (pH 5.1).
Injections: 100-μL of 100 μM thiourea in 0.25 M NH_4NO_3.
Waveforms: (PS-PCD) WF-3, (PCD) WF-2, (PAD) WF-1.

Fig. 6.
Demonstration of post-peak dips for detection of thiourea by PAD in 0.25 M NH_4NO_3 (pH 5.1).
Injections: 100 μM thiourea in 0.25 M NH_4NO_3.
Waveforms: WF-1.

Figs. 7A-7B
Current-potential curves for thiourea at a Au RDE vs. solution pH.
Solutions: (A) 0.25 M NH_4NO_3 (pH 5.1),
(B) 0.20 M NaOH (pH ca. 13).
Curves: (A,C) air sat'd. (B,D) N_2 sat'd.
(A,B) blank, (C,D) 0.20 mM thiourea.

Fig. 8.
Comparison of baseline shift for detection of thiourea in NH_4NO_3 by PS-PCD and PAD with a pH change from 3.8 to 5.1 (marked by arrow).
Injections: 100 μM thiourea in 0.25 M NH_4NO_3.
Waveforms: (PS-PCD) WF-3, (PAD) WF-1.

Figs 9A & 9B
Response for glucose at the Au RDE in 0.20 M NaOH (pH ca. 13).
Solutions: (A,C) blank, (B,D) 1.0 mM glucose.
Curves: (A,B) current vs. potential (i-E),
(C,D) charge vs. potential (q-E).

Fig. 10.
Comparison of flow-injection peaks for glucose and thiourea by PS-PCD with waveforms of Fig. 1.
Solutions: (A1,A2) 0.20 mM glucose in 0.20 M NaOH
(B1,B2) 0.10 mM thiourea in 0.20 M NaOH
Waveforms: (A1) WF-4, (A2) WF-5,
(B1), WF-4, (B2) WF-5.

Fig. 11.
Gradient liquid chromatographic separation and PAD using a pH reference of a complex mixture of amino acids.
Fig. 12.
Similar to Fig. 11 except for using PS-PCD.
Fig. 13.
Similar to Fig. 12 with improved chromatography.
Fig. 14.
Potential waveform used in connection with separation process of Figs. 12 and 13.

An improved variation of PCD will now be described in which the detection potential in the pulsed waveform is varied in a cyclic fashion during current integration. The cyclic potential change may be according to potential-sweep or potential-step functions, or a combination thereof, and the abbreviation PS-PCD is applied for the technique. The greatest significance for PS-PCD is anticipated for anodic detections based on oxide-catalyzed reactions, and it has been concluded that the technique is capable of virtual rejection of baseline drift in LC methods utilizing pH-gradient elution. The theory of gradient elution is well known and is described, for example, by Snyder and Kirkland in Introduction of Modern Liquid Chromatography, Second Edition, John Wiley & Sons, Inc. (1979), pp. 663-715, the details of which are hereby incorporated by reference.

Typical potential waveforms for PS-PCD are shown in Figs. 1B and 1C for comparison to the conventional waveform for PAD and PCD in Fig. 1A. In PS-PCD, the initial value of E_1 is chosen so that the electrode surface exists in an oxide-free state. Following a delay time of t_d, the detection potential is advanced to the value $E_{1'}$ by a fast potential sweep (Fig. 1B) or a potential step (Fig. 1C) for a time period of t_s. The value of $E_{1'}$ is chosen to cause the formation of surface oxide with the concurrent electrocatalytic oxidative reaction of soluble and/or adsorbed analyte. The detection potential then is returned to the initial value E_1 for the holding period t_h during which all oxide formed during the potential change to $E_{1'}$ is cathodically stripped from the electrode surface. The total time of the detection period is $t_1 = t_d + t_s = t_h$. An integrator (analog or digital) is activated during period t_d and remains active throughout period t_1. The output signal from the integrator is sampled at the end of period t_h and the value, or a proportional value, is fed to a recording device. Thereafter can be applied the positive and negative pulses to E_2 and E_3 which achieve anodic cleaning and cathodic reactivation, respectively. The integrator is reset to zero at the end of period t_3 just prior to the start of the next waveform cycle.

Background rejection in PS-PCD is achieved because the anodic charge for surface oxide formation ($q_{a,ox}$) during the potential change from E_1 to $E_{1'}$ is automatically compensated by the cathodic charge for oxide reduction ($q_{c,ox}$) with potential change from $E_{1'}$ to E_1. Background rejection is exact if $q_{c,ox} = - q_{a,ox}$. Sensitivity for analyte detection is greatest if the process is irreversible, i.e., no cathodic signal is obtained for reduction at E_1 of the products of the anodic detection reaction at $E_{1'}$. The value $E_{1'}$ is chosen to maximize the extent of oxidative reaction of soluble and absorbed analyte. However, $E_{1'}$ should not be so large positive to cause significant anodic solvent breakdown with evolution of O_2.

For the PS-PCD waveforms in Figs. 1B and 1C, the values of $E_{1'}$ and t_s can be sufficiently large to provide complete oxidative cleaning of the electrode and a subsequent step to E_2 for further oxidative cleaning may not be needed. The resulting waveform is shown in Fig. 1D. Advantages include a higher waveform frequency.

Solutions were prepared from Reagent Grade Chemicals (Fisher Scientific, Fair Lawn, NJ) and purified water (NANOpure II, Barnlsted Co., Boston, MA). Except where noted in voltammetric experiments, dissolved O_2 was removed by purging with pure N_2.

All data were obtained with a potentiostat (PAR 174A, EG&G Princeton Applied Research Corporation, Princeton, NJ) under computer control (Hewlett Packard, Palo Alto, CA) (5,12). The definitions of waveforms, as well as all other timing and switching operations, were under software control. The flow-injection (FI) system was based on a peristaltic pump (Minipuls HP4, Gilson Medical Electronics, Middleton, WI) and Teflon connecting tubing. The sample volumes injected were 100 µl and the flow rate was 0.5 ml min^{-1}. The electrochemical flow-through cell was of the "thin-layer" design (Dionex Corporation, Sunnyvale, CA) with a Au electrode (ca. 0.005 cm^2). A saturated calomel reference electrode (SCE) was substituted for the manufacturer supplied Ag/AgCl electrode (SSCE). Voltammetry was performed at a Au rotated disk electrode (RDE, 0.0050 cm^2) in a MSR rotator (Pine Instrument Co., Grove City, PA).

Voltammetry at the Au RDE was performed using a staircase waveform in which 20-mV steps were applied to the Model 174A to simulate a scan rate of ca. 4.8 V min^{-1}. Electrode current was measured during the last 16.7 ms of the time period for each step. Charge-potential (q-E) plots were obtained during staircase scans by continuous analog integration of electrode current.

The potential sweep from E_1 to $E_{1'}$ in waveform of Fig. 1B for PS-PCD was simulated by a staircase waveform using 30 mV steps initiated at the end of the delay time t_d. The detection response for the waveforms in Figs. 1C and 1D were found to be nearly equivalent to that in Fig. 1B for sulfur compounds. Hence, the waveform in Fig. 1D was used to obtain most of the PS-PCD data shown here. For waveforms shown in Figs. 1B-

1D, the integrator was activated at the start of period t_1. The sampling of electrode current in PAD and the accumulated charge in PCD and PS-PCD was achieved during a 16.7 msec period at the end of the detection period t_1. Detailed descriptions of the waveforms used to obtain data presented here are given in Table I on page 9a.

Staircase Voltammetry with Current Integration

Surfur compounds exhibit an anodic behavior at noble-metal electrodes which is under strong control by the simultaneous anodic formation of surface oxide (9, 10). This response is typified by the i-E plots shown in Fig. 2 (Curves B-D) which were obtained by staircase voltammetry obtained at a Au RDE rotated at 900 rev min^{-1} in 0.25 M NH_4NO_3 (pH 5.1) as a function of thiourea concentration. For comparison, the residual i-E plot obtained in the absence of thiourea is shown (Curve A). The surface-catalyzed anodic detection of thiourea is observed to occur simultaneously with the formation of

TABLE I

Description of Potential-Time Waveforms

WF-1	1A	PAD	E_1 = 1.00 V	t_d = 380 ms
				t_s = 16.7 ms
			E_2 = 1.20 V	t_2 = 300 ms
			E_3 = -0.60 V	t_3 = 500 ms
WF-2	1A	PCD	E_1 = 1.00 V	t_d = 0 ms
				t_s = 400 ms
			E_2 = 1.20 V	t_2 = 300 ms
			E_3 = -0.60 V	t_3 = 500 ms
WF-3	1D	PS-PCD	E_1 = 0.15 V	t_d = 100 ms
			E_1' = 1.20 V	t_s = 400 ms
				t_h = 300 ms
			E_2 = -0.60 V	t_2 = 500 ms
WF-4	1B	PS-PCD	E_1 = -0.10 V	t_d = 100 ms
			E_1' = 0.60 V	t_s = 800 ms
				t_h = 100 ms
			E_2 = -0.10 V	t_2 = 0 ms
			E_3 = -1.0 V	t_3 = 200 ms
WF-5	1D	PS-PCD	E_1 = -0.10 V	t_d = 100 ms
				t_s = 800 ms
			E_1' = 0.60 V	t_h = 100 ms
			E_2 = -1.00 V	t_2 = 500 ms

surface oxide during the positive potential sweep in the region ca. 0.6 - 1.3 V. Anodic solvent breakdown with

evolution of O_2 occurs at Au electrodes for E > ca. 1.3 V at pH 5.1. The anodic signal for thiourea decreases to zero on the negative sweep from 1.5 V when the rate of oxide formation goes to zero. Clearly, thiourea is reactive only with simultaneous formation of surface oxide and the oxide-covered Au electrode is inert for further anodic reaction of thiourea. The surface oxide formed during the positive potential sweep is cathodically reduced on the subsequent negative sweep to produce the cathodic peak in the region 0.5 - 0.2 V at pH 5.1. The optimum detection potential for PAD and PCD (E_1 in Fig. 1A) applied for thiourea at pH 5.1 in FI or LC system is in the range ca. 1.0 - 1.2 V, based on the appearance of a peak value for the anodic signal in the i-E plots of Fig. 2. For these values of detection potential, however, a large simultaneous background signal is obtained in PAD and PCD as a result of the formation of surface oxide.

The concept of PS-PCD is demonstrated for a slow triangular staircase potential sweep (4.8 V min^{-1}) at the Au RDE by the charge-potential (q-E) plots in Fig. 3 (curves C and D). THe simultaneous i-E data (curves A and B) obtained by staircase voltammetry are shown also to aid in the interpretation. The rotation speed was 1600 rev. min^{-1}. In the residual q-E plot for the absence of thiourea (curve C), a rapid buildup of charge occurs when oxide formation is initiated at ca. 0.7 V on the positive sweep and the accumulated charge returns to ca. zero starting at ca. 0.5 V on the negative sweep when the surface oxide is cathodically dissolved. In the presence of thiourea (curve D), the net charge remaining on the integrator after completion of the cyclic potential sweep corresponds to the contribution from the anodic reaction of thiourea.

Rate of Baseline Equilibration

The potential waveforms for PS-PCD (Figs. 1B-1D) incorporate a sampling methodology that can result in virtual rejection of the large background signals from oxide formation commonly observed in PAD and PCD. The anodic charge from oxide formation ($q_{a,ox}$) accumulated during the positive potential charge from E_1 to $E_{1'}$ is compensated by the nearly equivalent but opposite charge from the cathodic dissolution of the oxide ($q_{c,ox}$) for return of the potential from $E_{1'}$ to E_1.

The rate of equilibration and the drift of the baseline are compared in Fig. 4 for PS-PCD and PAD at a Au electrode in the FI system. The Au electrode was polished (0.5 μm alumina) prior to recording each response curve. The zero current for PAD is off the scale of Fig. 4. It is seen that severe baseline drift in PAD continues for longer than 10 min. This results from the gradual increase in the true electrode area during the detection process due to surface reconstruction caused by the repeated cycles of oxide formation and dissolution. With baseline rejection in PS-PCD, there is virtually no consequence evident from a charge in electrode surface area. Commonly for PS-PCD, the baseline is observed to reach its "zero" value within ca. 5-10 cycles of the waveform applied to a freshly polished electrode, as demonstrated in Fig. 4. Furthermore, deviation from this value over a several-hour period is less than or equivalent to the magnitude of the high frequency noise shown on the background signal. The equilibration rate and the extent of baseline drift for PS-PCD are virtually independent of the state of the electrode, i.e., whether the electrode has been "well-worked" or freshly polished. It is not necessary to polish electrodes used in PAD, PCD or PS-PCD. Electrodes can become very "tarnished" in appearance because of surface reconstruction after many months of operation; however, their response is not degraded.

A comparison is shown in Fig. 5 of the detection peaks for thiourea in 0.25 M NH_4NO_3 (pH 5.1) obtained by PS-PCD, PCD and PAD in the FI system. The full-scale current sensitivity of the stripchart recorder was adjusted from each detection mode so that the peak deflections would be equivalent. This allows for direct visual comparison of S/N factors in the figure. The magnitude of the baseline response is represented in the figure as a percentage of the net peak response. For example, the baseline signal for PS-PCD is only ca. 20% of the peak height for injections of 100 μM thiourea, whereas the baseline signal for PAD is nearly 150% the peak height. A small uncompensated baseline offset can persist in PS-PCD for three reasons: potential and current offsets in the operational amplifiers of the electronic instrument; a very short period for the second application of E_1 (i.e., period t_h), which does not permit complete cathodic removal of all surface oxide; and choice of an electrode material, electrode potentials (E_1 and $E_{1'}$ in Fig. 1B), and/or solution conditions for which $q_{c,ox} \neq -q_{a,ox}$.

Limits of Detection and Analytical Calibration

The detection limits for PS-PCD of sulfur compounds are superior to PAD and PCD, as would be anticipated from observation of the respective S/N values estimated from Fig. 5. The limit of detection (LOD) for thiourea by PS-PCD (S/N=3) was determined by flow injection to be ca. 2 μM for waveform WF-3 (see Table I), which corresponds to 15 ng in a 100-μl sample (0.15 ppm). The LOD for PAD (waveform WF-1) was 15 μM (110 ng, 1.1 ppm) and the LOD for PCD (waveform WF-2) was 6 μM (45 ng, 0.44 ppm). The calibration curve

for PS-PCD was linear over two decades in concentration (i.e., 2-200 μM). Note that the detection limits for PAD and PCD using the present "home-built" instrument are poorer than can be achieved using commercial instrumentation (Dionex Corp.). Hence, the values of LOD given here should be considered only for purposes of intercomparison of the three detection modes and not as indicators of values of LOD expected from state-of-the-art instrumentation.

Baseline Estimation in Flow-Injection Determinations

Current-potential curves obtained by staircase voltammetry at the Au RDE were shown in Fig. 2 as a function of thiourea concentration. Clearly, the apparent peak signal observed for cathodic dissolution of surface oxide ($q_{c,ox}$) decreases as thiourea concentration is increased. This is concluded to occur because the rate of oxide formation in inhibited substantially by the presence of absorbed sulfur and/or thiourea with the result that a smaller amount of surface oxide is produced during the positive potential sweep. This fact can have serious effects on the interpretation of i-t plots obtained for applications of PAD or PCD to flow-injection or chromatographic systems. The true baseline corresponding to the detection peak is not correctly estimated by extrapolation of the baseline observed immediately before or after the detection peak. Evidence of this effect is the appearance of the post-peak dips shown in Fig. 6 for injections of 100 μM thiourea. This demonstrates not only that less surface oxide is formed in the presence of adsorbed thiourea, but also that a finite amount of time (i.e., several waveform cycles) is required to completely clean and reactivate the electrode surface following passage of the sample bolus through the detector cell. For PS-PCD, there is no consequence of the variation in surface oxide coverage since the oxide formed as a result of the change from E_1 to $E_{1'}$ is subsequently cathodically dissolved following the potential change from $E_{1'}$ back to E_1 and the net integrated signal for this cyclic process remains at virtual zero regardless of changes in $q_{a,ox}$.

Effect of pH Change

To achieve minimal baseline in PS-PCD, it is essential that E_1 corresponds to a value at which the electrode is free of oxide and dissolved O_2 is not detected. Staircase voltammograms obtained at the Au RDE at 1600 rev min^{-1} are shown in Fig. 7A for thiourea in 0.25 M NH_4NO_3 (pH 5.1) and in Fig. 7B for 0.20 M NaOH (pH ca. 13). As a result of the change in pH from 5.1 to 13, the peak potential for oxide stripping at the Au electrode shifts negative by ca. 0.40 V, whereas the half-wave potential for O_2 reduction shifts by only ca. 0.15 V. Hence, for high values of pH, it becomes impossible to locate a value for E_1 in the PS-PCD waveform (Figs. 1B-1D) such that all surface oxide is cathodically dissolved but for which dissolved O_2 is not detected. The value -0.15 V at pH 13 is only marginally successful, and application of PS-PCD to Au electrodes in alkaline solutions containing dissolved O_2 is limited to pH < ca. 13.

It is important also that the range of the potential change from E_1 to $E_{1'}$ is chosen to span the majority of the voltammetric region for surface oxide formation; however, $E_{1'}$ should not exceed values for onset of significant evolution of O_2. From the i-E curves in Fig. 7, it is observed that the onset of anodic O_2 evolution is shifted negative by ca. 0.40 V for the change in pH from 5 to 13. Clearly, it is impossible to design a waveform for successful PS-PCD at pH 5 which will apply satisfactorily at pH 13 without adjustment of all values of potential in the waveform.

Peaks for thirourea obtained by PS-PCD and PAD are compared in Fig. 8 for flow-injection detections with a pH step in the carrier solution from 3.8 to 5.1, as designated by the arrow. The recorder setting for each experiment was adjusted such that the peak deflection would be nearly equivalent for the two detection techniques. For PS-PCD, the change in baseline response is very small, whereas the baseline shift for PAD is much more severe. The sensitivity for thiourea detection by either method exhibits little variation with the change in solution pH. Also, it is readily apparent that the S/N is superior for PS-PCD.

Consideration of Carbohydrate Detection

Monosaccharides and disaccharides exhibit a nearly mass transport-limited peak-shaped response at a Au electrode in alkaline solutions (5). As shown for the positive potential sweep in the voltammetric curves in Fig. 9 obtained at the Au RDE at 900 rev min^{-1}, the anodic peak for glucose is obtained in a potential region where no substantial quantity of surface oxide is formed (compare curves A and B). Even though the voltammetric peak response for glucose is virtually mass-transport controlled, detection at a constant potential without the benefit of the cleaning, and activation pulses in PAD or PCD is unsatisfactory. For detection at constant potential, the anodic response for carbohydrates decays steadily at Au electrodes. The loss of surface activity is concluded to be the result of the accumulation of absorbed products of the detection reaction. A similar ob-

servation at Pt electrodes led to the original motivation for the development of PAD (1). As shown by curve B in Fig 9 (positive sweep), oxidation of the carbohydrate ceases concurrently with the onset of oxide formation at ca. 0.2 V. The peak signal superimposed on the oxide formation wave (0.25-0.5 V) in the presence of carbohydrates corresponds to the oxide-catalyzed oxidative desorption of the absorbed carbonaceous material. The basis of PS-PCD for carbohydrates is illustrated by the Q-E plots for glucose in Fig. 9 (curves C and D) obtained with the slow triangular staircase sweep (4.8 V min^{-1}).

For carbohydrates under highly alkaline conditions, it is not possible to choose values of E_1 and $E_{1'}$ which encompass the entire detection peak without the simultaneous detection of dissolved O_2. This observation, plus the knowledge that a minimal background current is observed in determinations of carbohydrates by PAD and PCD, because oxide is not formed at the detection potential, leads to the conclusion that there is not likely to be a significant improvement in detectability for carbohydrates by PS-PCD in comparison to PCD in solutions of pH > ca. 11. Furthermore, sensitivity for carbohydrates decreases rapidly for pH < 11.

Comparison of Waveforms

The optimization of the waveform for PS-PCD, e.g., choice of Fig. 1B vs. Figs. 1C or 1D, is influenced by the analyte(s) of interest. For analytes whose detection is inhibited by formation of surface oxide, e.g., carbohydrates (see Figs. 9A and 9B), the waveform depicted in Figs. 1C and 1D are not considered appropriate because the stepwise change of potential from E_1 to $E_{1'}$ results in the rapid and extensive formation of oxide with cessation of analytical response (see Fig. 9). Absorbed analytes detected by mechanisms which are catalyzed by formation of surface oxide, e.g., sulfur compounds, are expected to be detected well by either waveform. Results from a comparison of the waveforms in Figs. 1B and 1D are shown in Fig. 10 for detection of glucose (A1, A2) and thiourea (B1, B2) in 0.2 M NaOH. For the comparison, the total period of detection was the same in the two waveforms (1000 ms). Numerical values for the baseline signal (μC) are indicated in parentheses. Glucose shows a substantially higher sensitivity for the waveform in Fig. 1B as compared to Fig. 1D, as predicted. Thiourea is detected with similar sensitivity, also as predicted. As was the case for thiourea, amino acids also are detected by processes which are catalyzed by the formation of the surface oxides, as will be described in conjunction with Figs. 11-13.

Fig. 11 contains a chromatogram for 17 amino acids (peak identity given on page 17a) using the Dionex scheme for gradient elution with detection by PS-PCD. The chromatographic column was the Dionex AS-8. The tremendous shift in baseline is typical for PAD or PCD detection of amino acids when the gradient elution method is used, i.e., the composition of the mobile phase is caused to change during the elution process. Note it is apparent that some of the detection peaks are lost in the shifting baseline. This particular chromatogram was obtained using the pH electrode as the reference. If the SCE reference had been used, the baseline shift would have been even more severe.

Fig. 12 contains a chromatogram obtained under the exact conditions of Fig. 11 except that PS-PCD was used for detection, with the pH reference. It is very evident that the great significance of the invention is the stability of the baseline when gradient elution is employed. Peak identity given on page 17b.

Fig. 13 contains a chromatogram obtained with the PS-PCD and pH reference with a slight change in the gradient elution conditions. The different conditions allowed separation of 20 amino acides. Again, the baseline is remarkably stable. Peak identity given on page 17c.

Fig. 14 shows the potential waveform for the PS-PCD separation process of Figs. 12 and 13, and page 17d shows a Table illustrating a solvent system for amino acid separation.

LC-PCD of the Pierce protein hydrolyzate using a glass reference electrode

Electrode:	Au, glass reference
Column:	AS-8
Solutions:	see Table III
Samples:	Pierce protein hydrolyzate, 5 x 10^{-4} M each, except cystine at 2.5 x 10^{-4} M

1) arginine	10) leucine
2) lysine	11) methionine
3) threonine	12) histidine
4) alanine	13) phenylalanine
5) glycine	14) glutamic acid
6) serine	15) aspartic acid
7) valine	16) cystine
8) proline	17) tyrosine
9) isoleucine	

Waveform:

E1: 200	E2: 800	E3: 200	E4: 1000	E5: -350
Ta: 350	Tb: 50	Tc: 5	Td: 1	Te: 344
Tf: 50	Tg: 10	Th: 100	Ti: 90	

LC-PCD of 20 amino acids

Electrode: Au, glass reference
Column: AS-8
Solutions: see Table III

Samples:

1) arginine	11) isoleucine
2) lysine	12) leucine
3) glutamine	13) methionine
4) asparagine	14) histidine
5) threonine	15) phenylalanine
6) alanine	16) glutamic acid
7) glycine	17) aspartic acid
8) serine	18) cysteine
9) valine	19) cystine
10) proline	20) tyrosine

Waveform:

E1: 200	E2: 800	E3: 200	E4: 1000	E5: -350
Ta: 350	Tb: 50	Tc: 5	Td: 1	Te: 344
Tf: 50	Tg: 10	Th: 100	Ti: 90	

Table III. Solvent system for amino acid separation with the Dionex AS-8 column

Solution #1 (regenerant):	0.56 M NaOH/ 0.64 M boric acid
Solution #2:	0.023 M NaOH/ 0.007 M $Na_2B_4O_7$ (0.005 M $Na_2B_4O_7$ substituted for LC-PAD and LC-PCD)
Solution #3:	0.08 M NaOH/ 0.018 M $Na_2B_4O_7$/ 2% MeOH
Solution #4:	0.4 M NaOAc/ 0.001 M NaOH/ 2% MeOH

Flow rate = 1.0 ml min^{-1}

Gradient program

Time (min)	Sol #1 %	Sol #2 %	Sol #3 %	Sol #4 %	inj val pos
0.0	-	100	-	-	inj
4.0	-	100	-	-	inj
4.1	100	-	-	-	inj
13.9	100	-	-	-	inj
14.0	-	100	-	-	inj
25.8	-	100	-	-	load
26.0	-	100	-	-	inj
36.0	-	100	-	-	inj
40.0	-	-	100	-	inj
46.0	-	-	100	-	inj
46.1	-	-	90	10	inj
56.0	-	-	-	100	inj

The design of the waveform for PS-PCD at a Au electrode can result in virtual elimination of baseline signals for oxide-catalyzed detection processes, and the technique is recommended in conjunction with a pH reference for liquid chromatographic separations which utilize pH-gradient elution over a limited pH range.

It should be clearly understood that the technique according to the present invention is for electrochemical detection of analyte in a liquid chromatographic environment.

The use of PS-PCD with a Au working electrode has been described, but this technique will work equally

well with other electrode substrates, such as Pt, Ru, Rh, Pd, Pb, etc., for which an oxide layer can be formed and subsequently stripped at more cathodic potentials.

In general, this technique is applicable to the measurement of irreversible electrochemical processes superimposed or coincident with irreversible processes. the measurement of surface-oxide catalyzed reactions during the formation of surface oxide is a single example of the PS-PCD technique.

The PS-PCD technique is believed applicable to detection of compounds such as amino acides, carbohydrates and sulfur compounds. The PS-PCD technique is applicable to the detection of alcohols, polyalcohols, amines, alkanolamines, monosachrides, disachrides, oligosachrides, glycopeptides, glycoproteins, thiocarbonides, theophosphates and inorganic sulfur.

As described herein, the PS-PCD method of the present invention is particularly applicable to detection of multiple chemical components in a liquid sample which have been separated by liquid chromatography, particularly high performance liquid chromatography (HPLC). The liquid sample is normally mixed with an eluent including an electrolyte as a developing reagent and passed through a chromatography column. The packing for the column typically would include gel or particulate forms of ion exchange or reverse phase packing. The technology is well developed. For example, see C.F.Simpson, Techniques of Liquid Chromatography, 1983, J.H. Knox, High Performance Liquid Chromatography, 1981, and K. Polkar et al., Liquid Chromatography in Clinical Analysis, 1981.

In addition, the PS-PCD method is useful as a method of detection in flow injection analysis (FIA). Such systems are described in Skeggs, Amer. J. Clin. Path., 28, 311-322 (1957) and in the U.S. patents 4,013,413, 4,022,575, 4,177,677, 4,224,033, 4,227,973, 4,314,824, 4,315,754, 4,352,780, 4,399,102, 4,399,255, and 4,504,443. In such systems, these samples are supplied to the detector in a continuous liquid carrier flow rather than by being separated, e.g., in liquid chromatography. This technique is of limited application in comparison to the aforementioned liquid chromatographic system.

REFERENCES

1. Hughes, S., Johnson, D.C. Anal.Chim.Acta 1981, 132, 11.
2. Hughes, S., Johnson, D.C. Anal.Chim.Acta 1983, 149, 1.
3. Edwards, P., Haak,K. Amer,Lab, 1983, April 78.
4. Rocklin, R.D., Pohl,C.A. J.Lig.Chromatogr. 1983, 6(9), 1577.
5. Neuburger, G.G., Johnson, D.C. Anal.Chem. 1987, 59, 150.
6. Neuburger, G.G., Johnson, D.C. Anal.Chem. 1987, 59, 203.
7. Polta, J.A., Johnson, D.C. J.Lig.Chromatogr., 1983, 6, 1727.
8. Polta, J.A., Johnson, D.C., Merkel, K.E. J.chromatogr. 1985, 324, 407.
9. Polta, T.Z., Johnson, D.C. J.Electroanal.Chem. 1986, 209, 159.
10. Polta, T.Z., Luecke,G.R., Johnson, D.C. J.Electroanal.Chem. 1986, 209, 171.
11. Thomas, M.B., Sturrock, P.E. J.Chromatogr. 1986, 357, 318.
12. Neuburger, G.G., Johnson, D.C. Anal.Chim.Acta 1987, 192, 205.
13. Polta, J.A., Yeo, I.H., Johnson, D.C. Anal.Chem. 1985, 57, 563.
14. Mead, D.A., M.S.Dissertation, Iowa State University, Ames, IA., 1988.
15. CH-A-659,327 A5, J. B. Vasiliev, et al.

Claims

1. A liquid chromatographic pulsed coulometric detection method for direct detection of at least one analyte, comprising the following steps:
   applying an electric potential waveform defining a potential sweep or potential step function to a working electrode in a flow-through cell, and
   electrochemically detecting analyte directly by integrating current over a cyclic detection portion of the total electric potential waveform.

2. The method as claimed in claim 1 wherein said flow-through cell is a three electrode cell and wherein one of the electrodes is a pH reference electrode.

3. The method as claimed in claim 2 wherein pH gradient elution is employed.

4. The method as claimed in claim 1 further including the steps of:

generating multi-step potential waveforms having cyclic potential changes where the cyclic waveforms have a first initial potential value (E_1) for a first time period t_d so that surfaces of said working electrode exist in an oxide-free state;

advancing the potential value to a second, higher value (E'_1) for a time period t_s so as to cause on said working electrode the formation of surface oxide with concurrent electrocatalytic oxidative reaction of soluble and/or absorbent analyte; and

returning the potential value to said first value E_1 for a holding time period t_h, during which all oxide formed during the potential change to E'_1, is cathodically stripped from said surfaces of said working electrode.

5. The method as claimed in claim 4, wherein the cyclic potential change is advanced according to a potential sweep function.

6. The method as claimed in claim 4, wherein the cyclic potential change is advanced according to a potential step function.

7. The method as claimed in claim 4, including the further step of advancing said potential value to a value E_2 higher than said first or second values for a period of time t_2 for oxidative cleaning of said surfaces of said working electrode.

8. The method as claimed in claim 4 or 7, including the further step of decreasing said potential value to a value E_3 lower than said first value for a time period t_3 for reactivation by cathodic dissolution of the surface oxide formed at E_1, and/or E_2.

Patentansprüche

1. Chromatographisches gepulstes coulometrisches Flüssigkeits-Erfassungsverfahren zur direkten Erfassung wenigstens eines Analyten mit folgenden Schritten:

Anlegen eines elektrischen Potentialsignals, das eine Potentialkipp- oder Potentialstufen-Funktion an eine Arbeitselektrode in einer Durchflußzelle definiert, und

elektrochemisches Erfassen des Analyten direkt durch Integrieren des Stromes über einen zyklischen Erfassungsbereich des gesamten elektrischen Potentialsignals.

2. Verfahren nach Anspruch 1, wobei die Durchflußzelle eine Zelle mit drei Elektroden ist und wobei eine der Elektroden eine pH-Wert-Bezugselektrode ist.

3. Verfahren nach Anspruch 2, wobei eine pH-Gradienten-Elution benutzt wird.

4. Verfahren nach Anspruch 1 mit folgenden weiteren Schritten:

Erzeugen mehrstufiger Potentialsignale mit zyklischen Potentialänderungen, wobei die zyklischen Signale einen ersten Anfangspotentialwert (E_1) für eine erste Zeitperiode t_d haben, so daß Oberflächen der Arbeitselektrode in einem oxidfreien Zustand existieren,

Erhöhen des Potentialwertes auf einen zweiten, höheren Wert (E'_1) für eine Zeitperiode t_s, so daß auf der Arbeitselektrode Oberflächenoxid mit gleichzeitiger elektrokatalytischer Oxidationsreaktion eines löslichen und/oder absorbierenden Analyten gebildet wird, und

Zurückführen des Potentialwertes auf den ersten Wert (E_1) für eine Halte-Zeitperiode t_h, während der alles während der Potentialänderung auf E'_1 gebildete Oxid kathodisch von den Oberflächen der Arbeitselektrode abgezogen wird.

5. Verfahren nach Anspruch 4, wobei die zyklische Potentialänderung nach einer Potential-Kippfunktion erhöht wird.

6. Verfahren nach Anspruch 4, wobei die zyklische Potentialänderung nach einer Potential-Schrittfunktion erhöht wird.

7. Verfahren nach Anspruch 4 weiter mit dem Schritt des Erhöhens des Potentialwertes auf einen Wert E_2, der höher ist als der erste oder zweite Wert, für eine Zeitperiode t_2 zum oxidierenden Reinigen der Oberflächen der Arbeitselektrode.

8. Verfahren nach Anspruch 4 oder 7 mit dem weiteren Schritt des Verminderns des Potentialwertes auf einen Wert E_3, der kleiner ist als der erste Wert, für eine Zeitperiode t_3 zur Reaktivierung durch kathodische Auflösung des bei E_1 und/oder E_2 gebildeten Oberflächenoxids.

Revendications

1. Procédé de détection coulométrique pulsée chromatographique liquide destiné à la détection directe d'au moins un analyte, comprenant les étapes suivantes consistant à:
appliquer une forme d'onde de potentiel électrique définissant une fonction de balayage de potentiel ou d'échelon de potentiel à une électrode en fonctionnement dans une cellule à recirculation, et
détecter électrochimiquement l'analyte directement en intégrant le courant sur une partie cyclique de détection de la forme d'onde totale du potentiel électrique.

2. Procédé selon la revendication 1, dans lequel ladite cellule à recirculation est une cellule à trois électrodes et dans lequel une des électrodes est une électrode de référence de pH.

3. Procédé selon la revendication 2, dans lequel l'élution du gradient de pH est employée.

4. Procédé selon la revendication 1, comprenant en outre les étapes consistant à:
générer des formes d'ondes de potentiel à échelons multiples possédant des variations cycliques de potentiel lorsque les formes d'ondes cycliques ont une première valeur de potentiel initiale (E_1) durant un premier intervalle de temps t_d, de sorte que les surfaces de ladite électrode en fonctionnement se trouvent sans oxyde;
amener la valeur de potentiel à une seconde valeur supérieure (E') durant un intervalle de temps t_s, de façon à provoquer sur ladite électrode en fonctionnement la formation d'oxyde de surface à l'aide d'une réaction d'oxydation électrocatalytique en parallèle d'un analyte soluble et/ou absorbant; et
ramener la valeur de potentiel à ladite première valeur E_1 durant un intervalle de temps d'arrêt t_h pendant lequel tout l'oxyde formé pendant la variation de potentiel en E' est ôté par voie cathodique desdites surfaces de ladite électrode en fonctionnement.

5. Procédé selon la revendication 4, dans lequel la variation cyclique de potentiel est amenée selon une fonction de balayage de potentiel.

6. Procédé selon la revendication 4, dans lequel la variation cyclique de potentiel est amenée selon une fonction d'échelon de potentiel.

7. Procédé selon la revendication 4, comprenant en outre l'étape consistant à amener ladite valeur de potentiel à une valeur E_2 supérieure auxdites première et seconde valeurs durant un intervalle de temps t_2 afin de nettoyer par oxydation lesdites surfaces de ladite électrode en fonctionnement.

8. Procédé selon la revendication 4 ou 7, comprenant en outre l'étape consistant à abaisser ladite valeur de potentiel à une valeur E_3 inférieure à ladite première valeur durant un intervalle de temps t_3 afin de réactiver, par dissolution par voie cathodique, l'oxyde de surface formé en E' et/ou E_2.

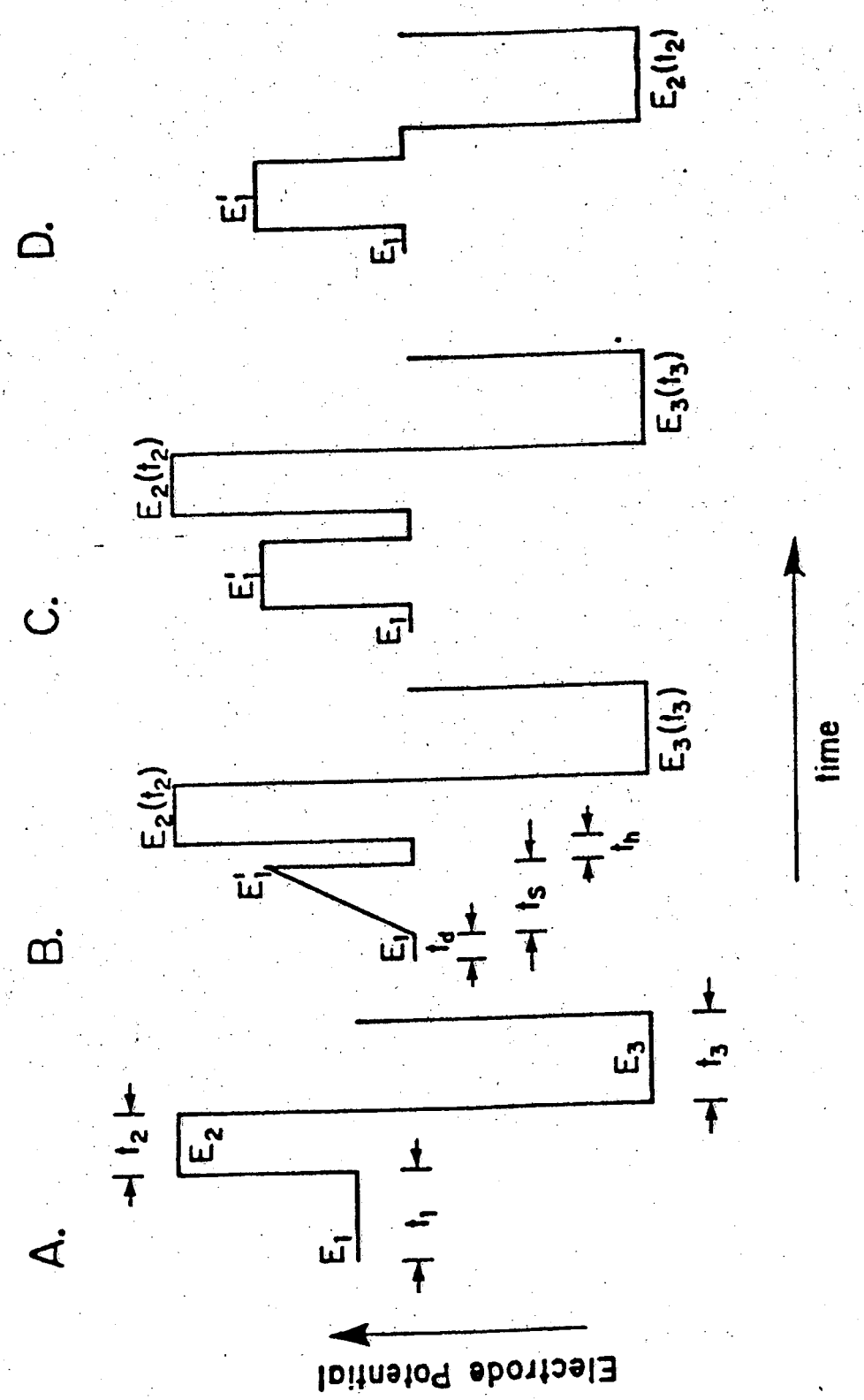
A.
B.
C.
D.
Electrode Potential
time
E1
E2
E3
E1'
E2(t2)
E3(t3)
t1
t2
t3
td
ts
th

Figure 1.

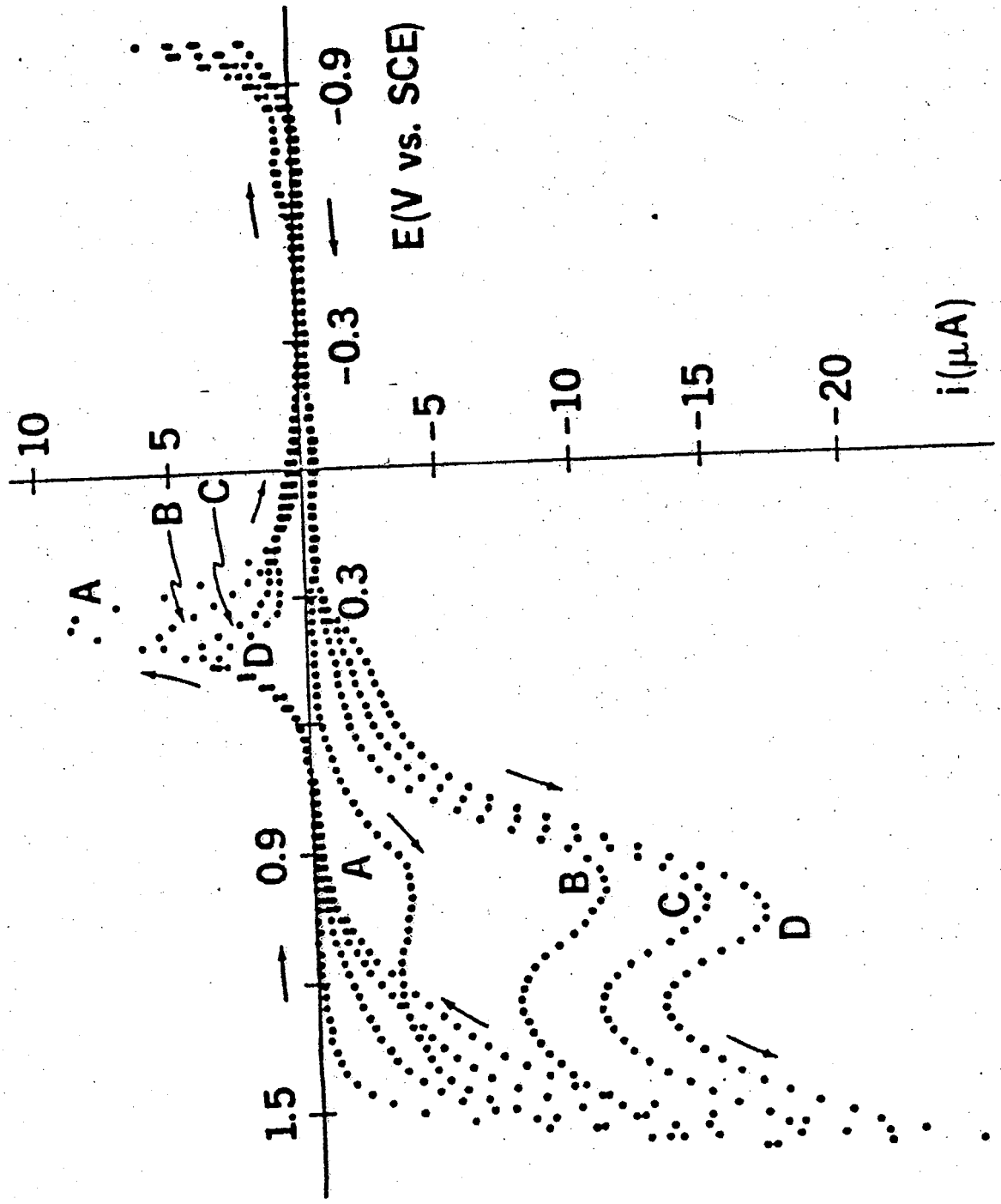

Figure 2.

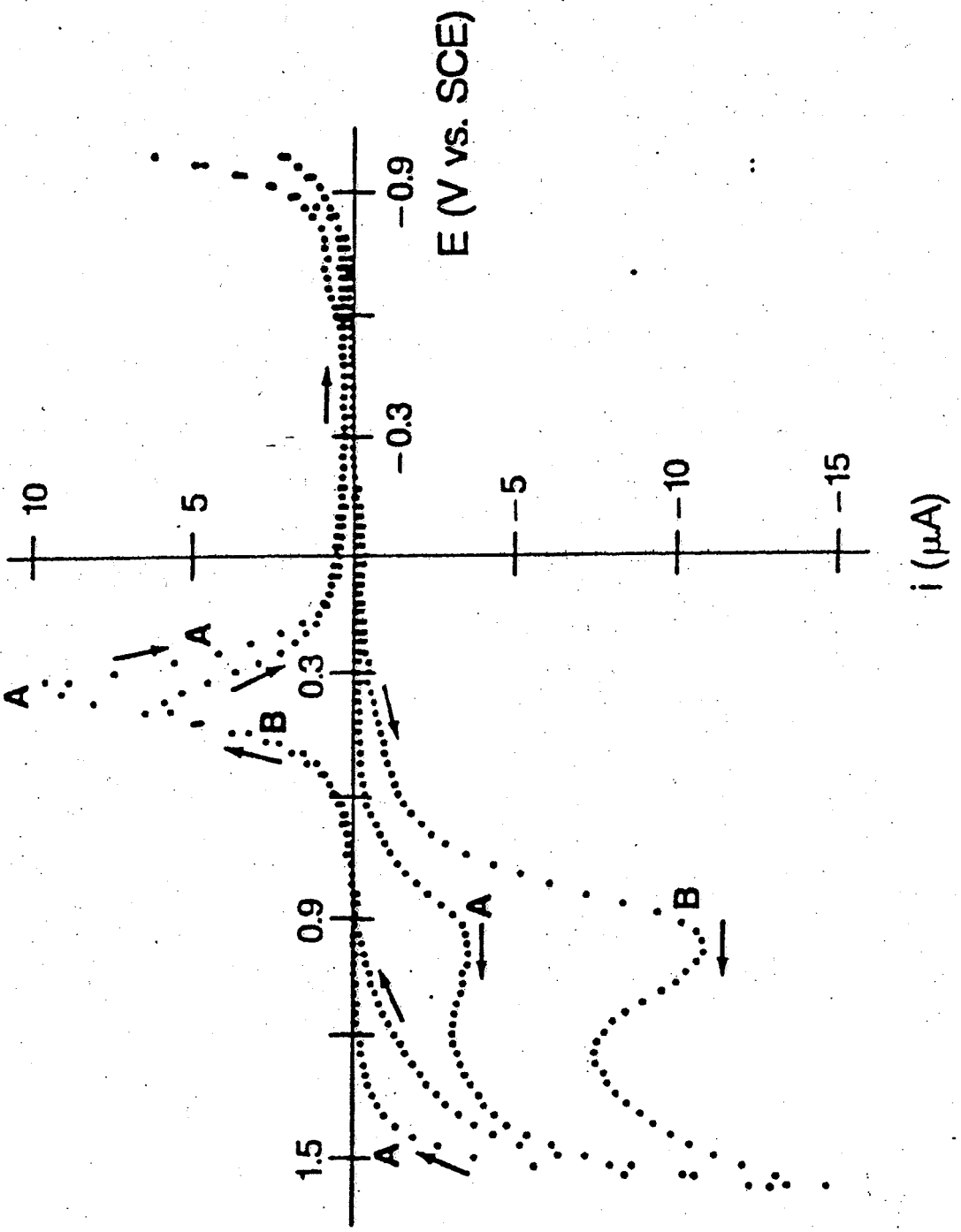

Figure 3A

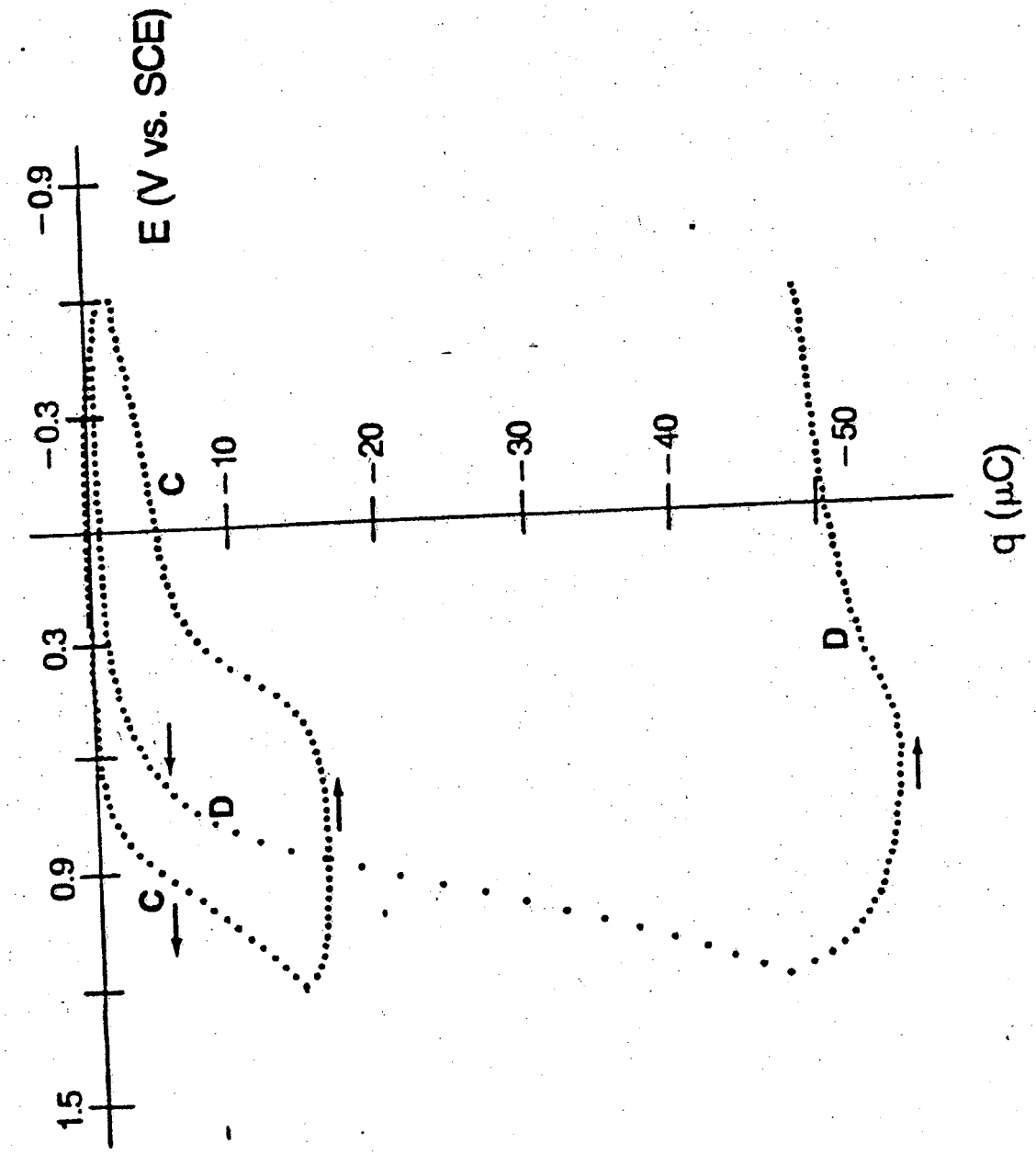

Figure 3B

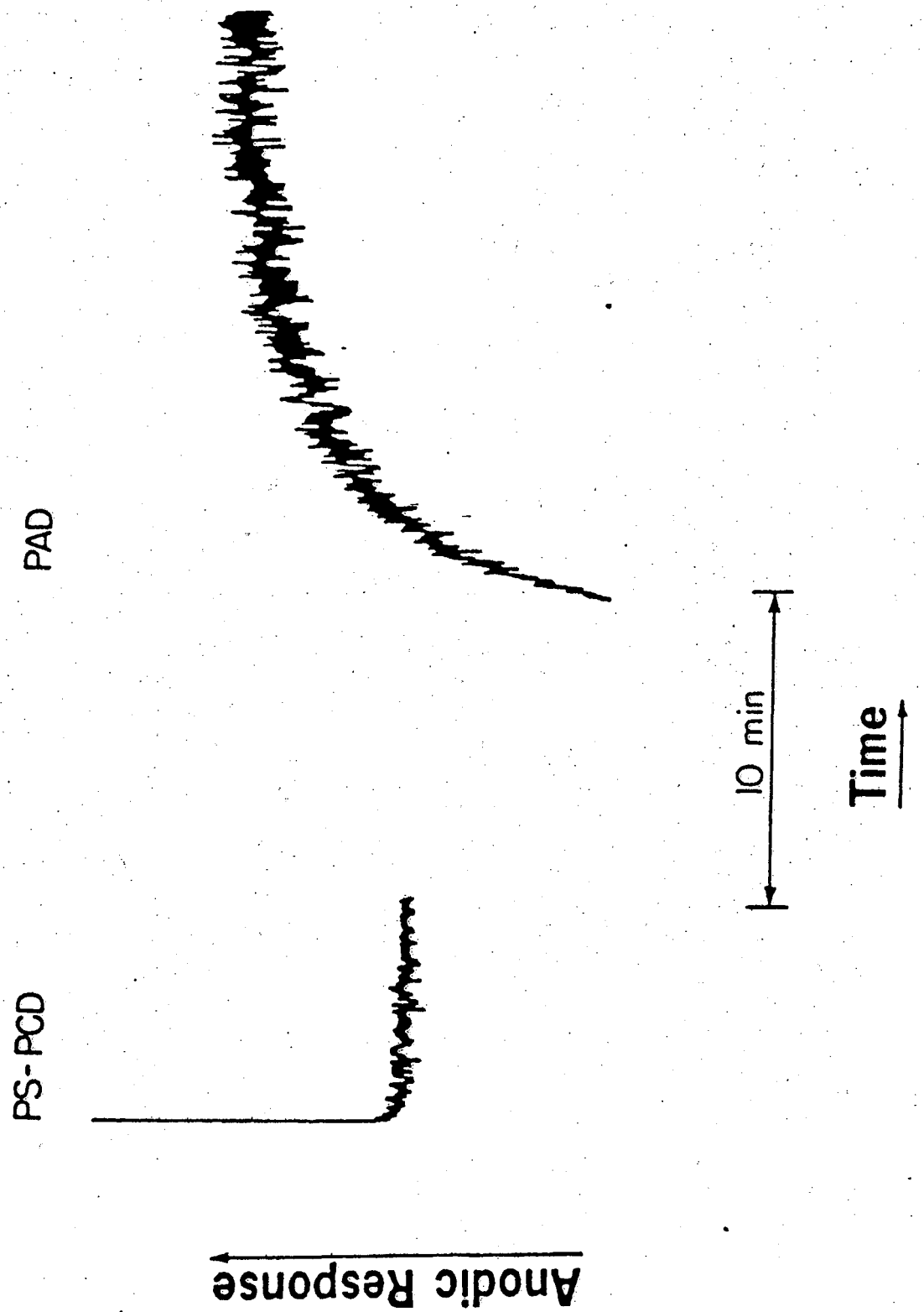

Figure 4.

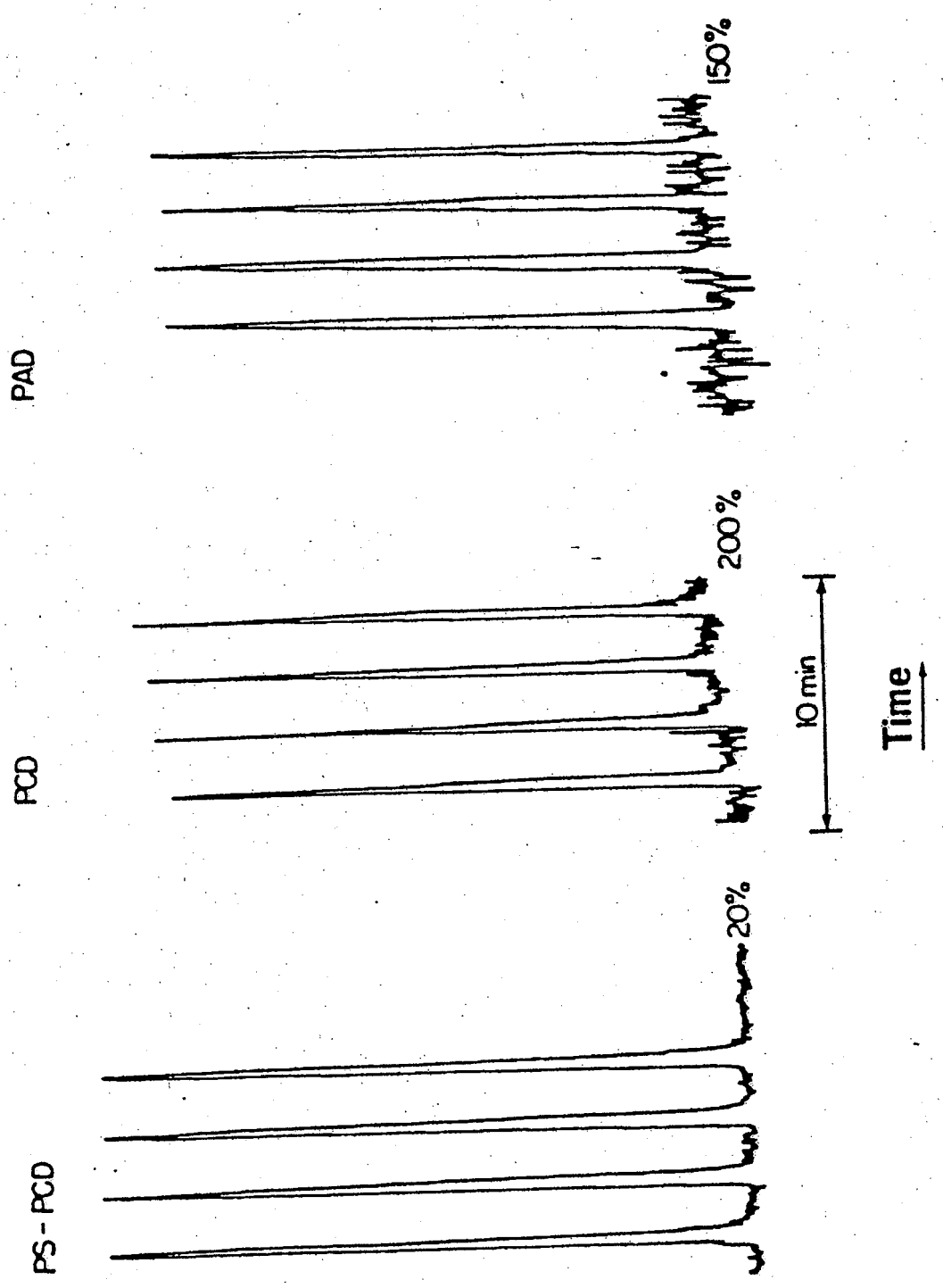

Figure 5.

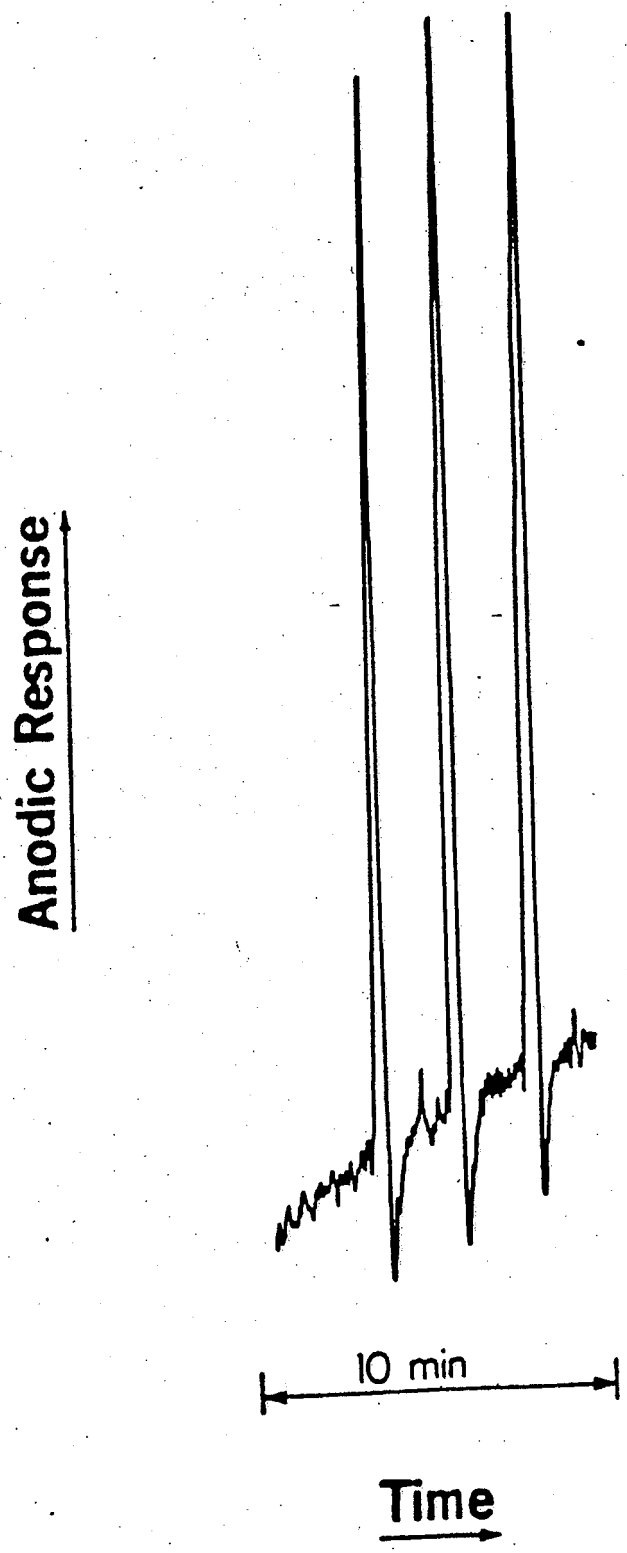
Anodic Response
10 min
Time

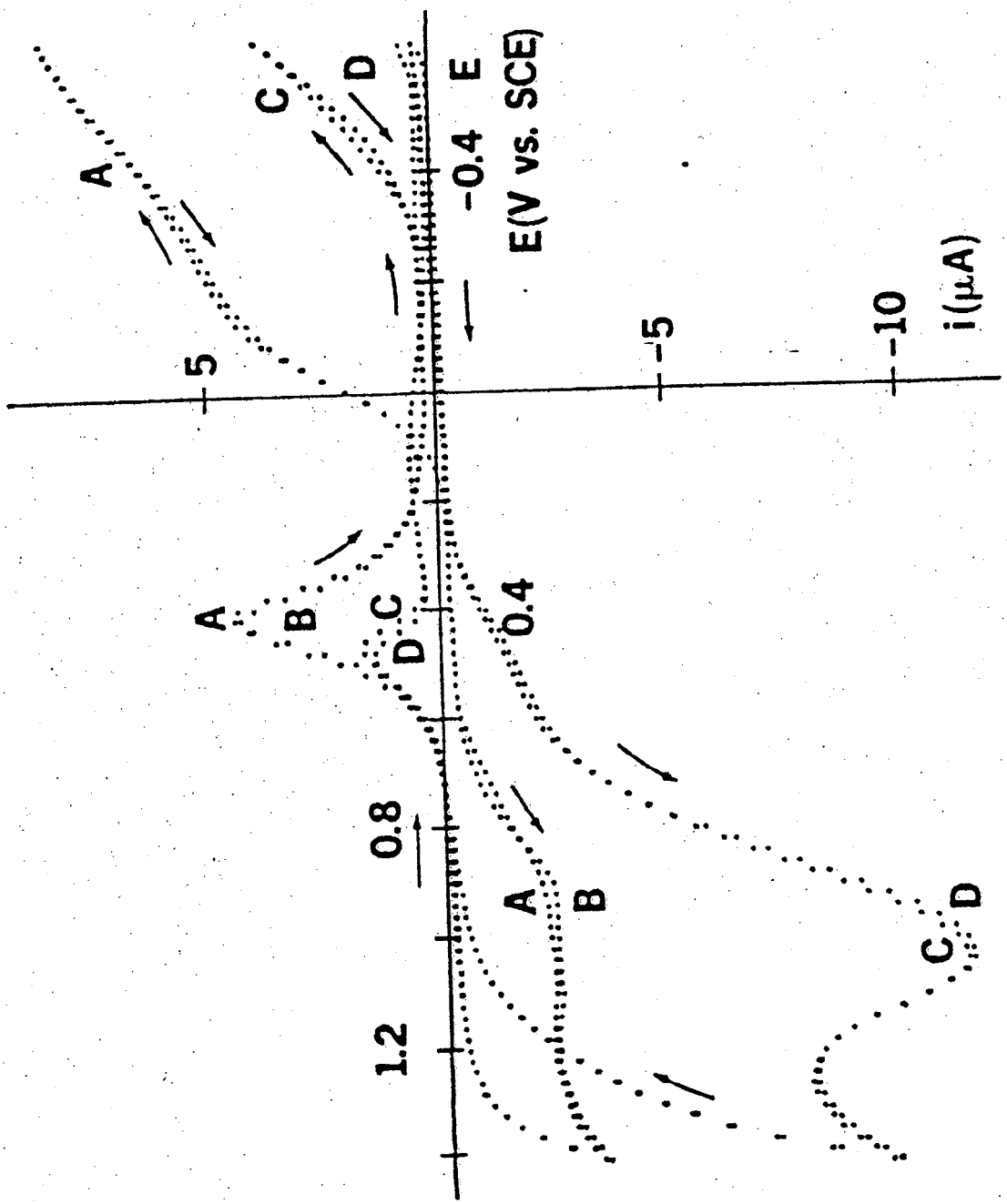

Figure 7A.

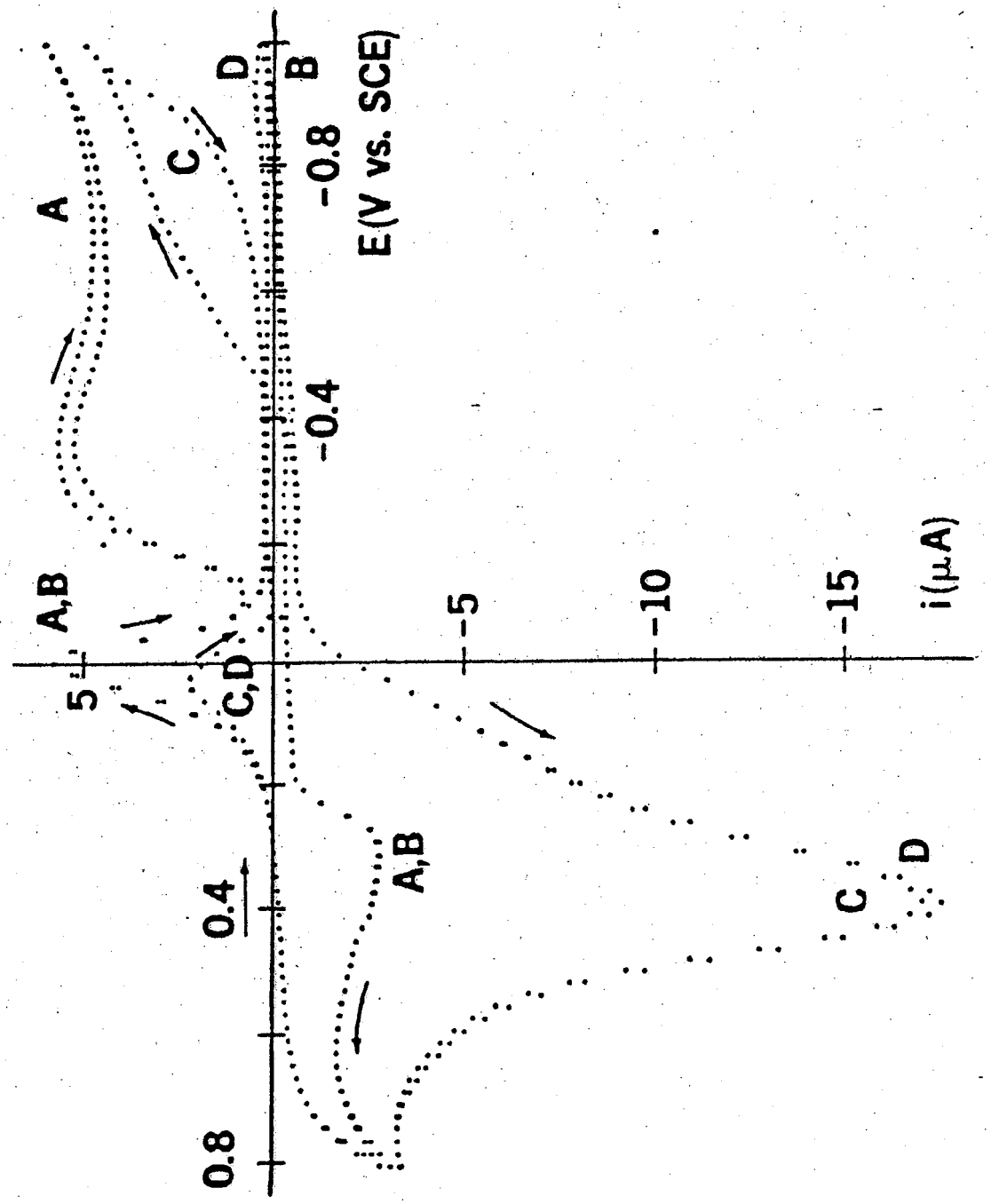

Figure 7B.

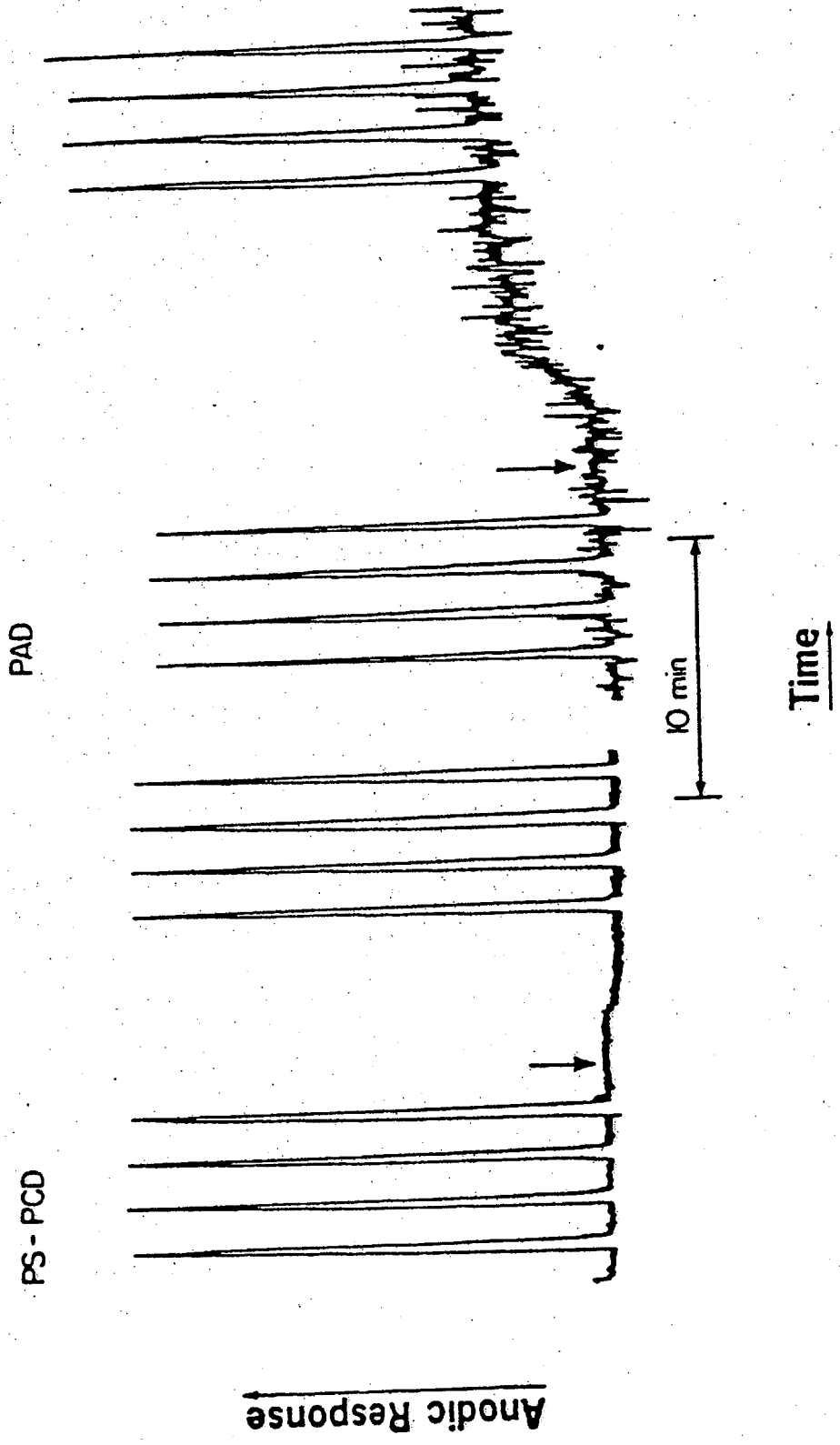

Figure 8.

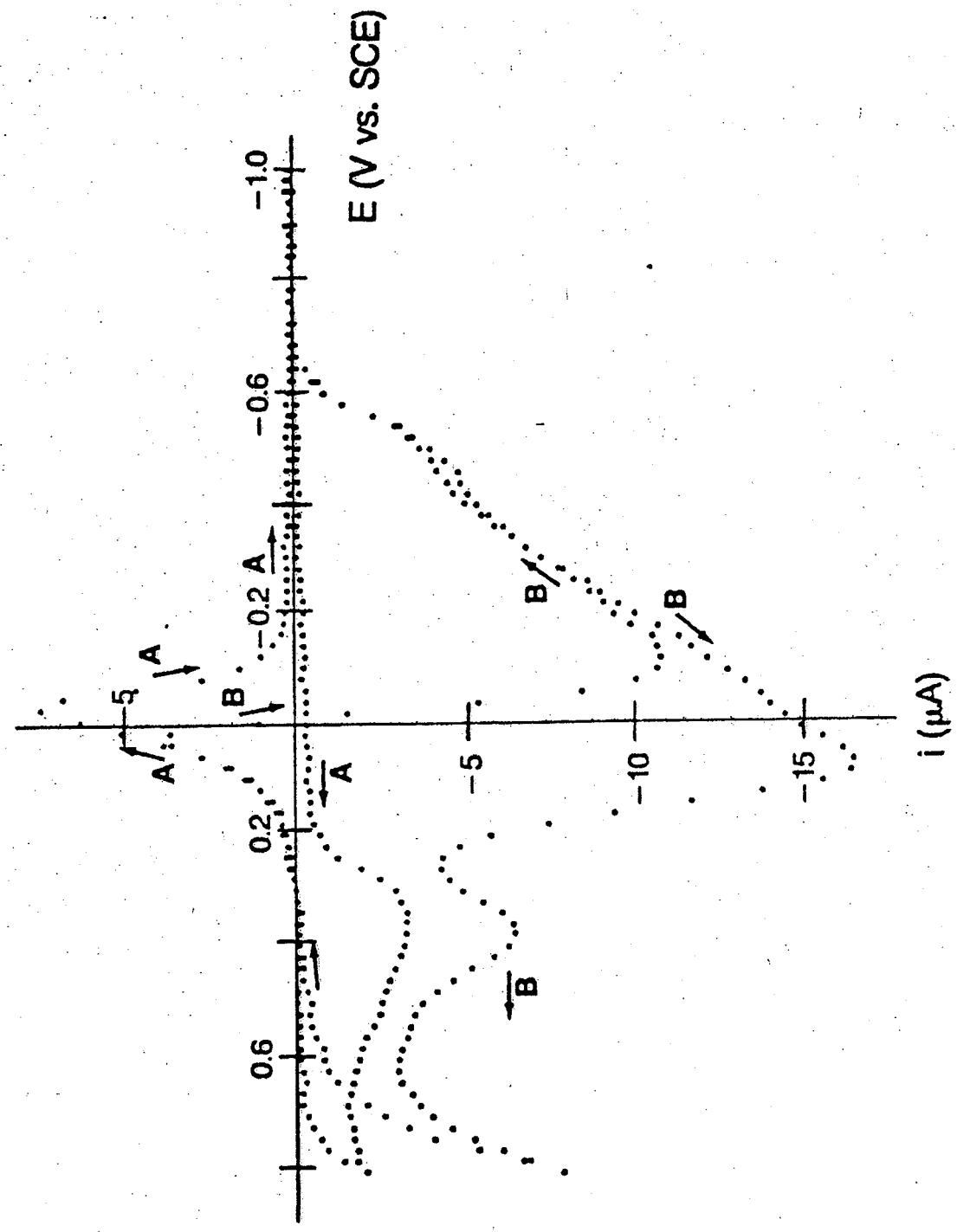

Figure 9A

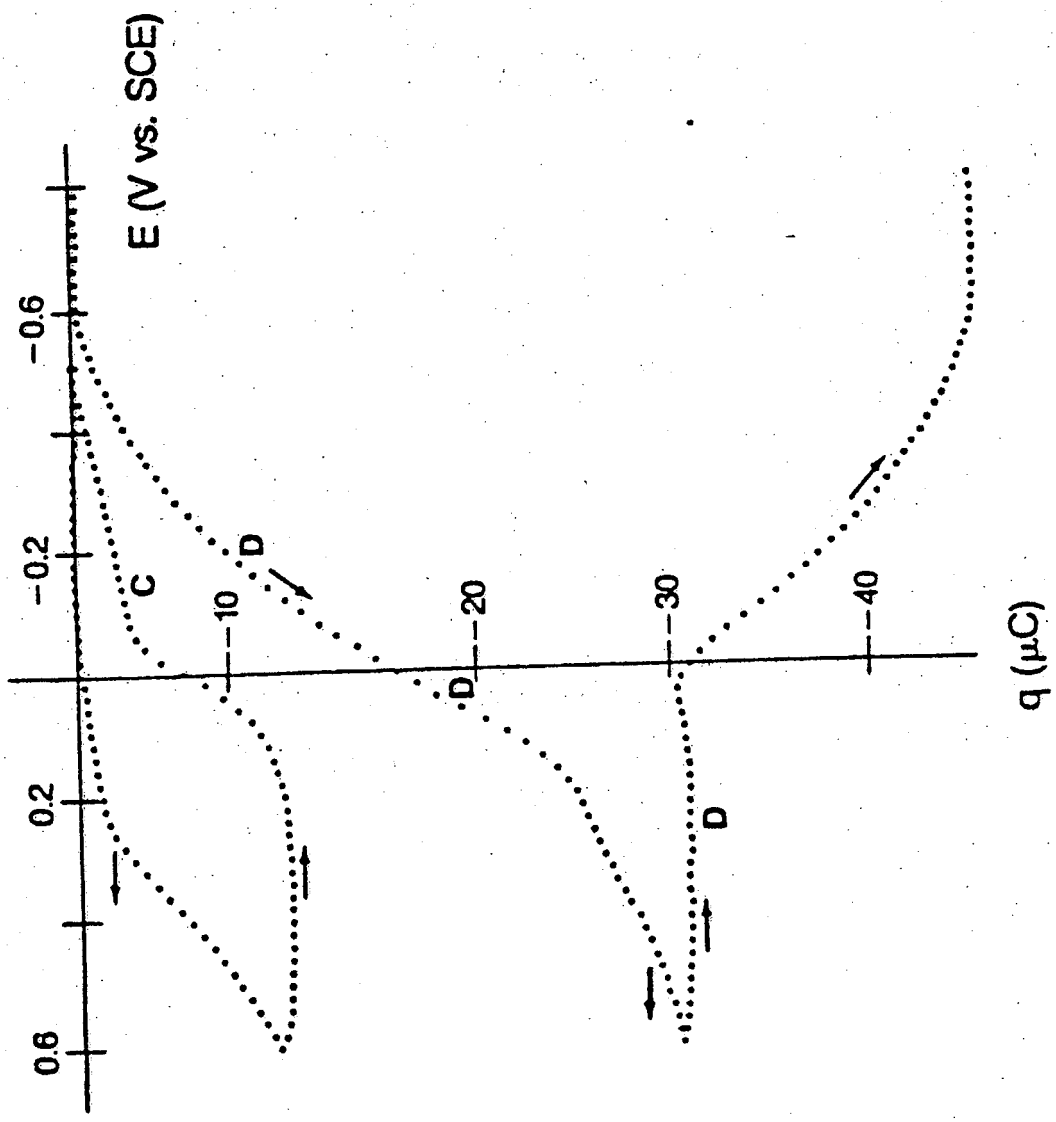

Figure 9B

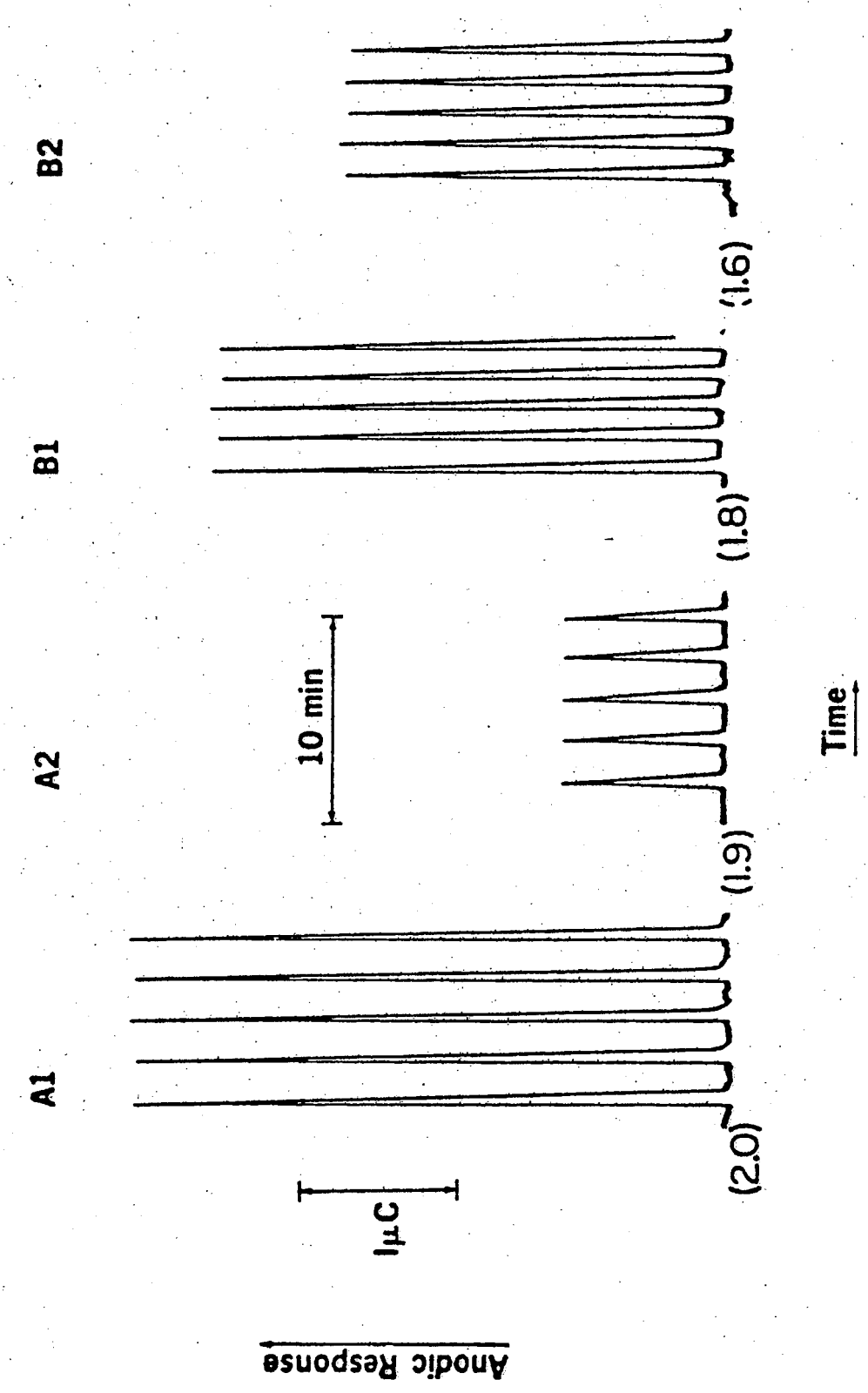

Figure 10.

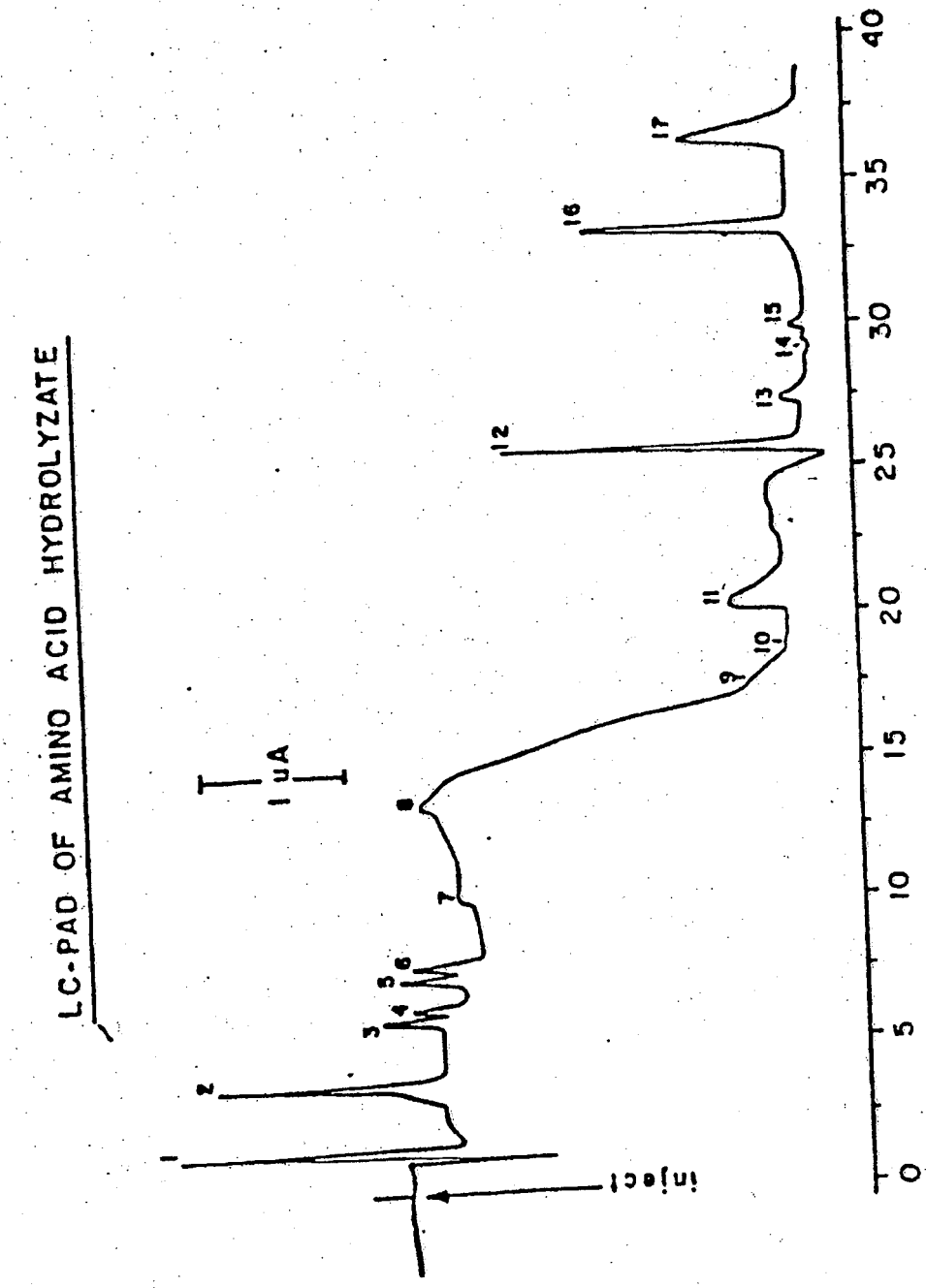
LC-PAD OF AMINO ACID HYDROLYZATE
1 uA
inject
TIME (min.)
0
5
10
15
20
25
30
35
40
2
3
4
5
6
7
8
9
10
11
12
13
14
15
16
17

FIG 11

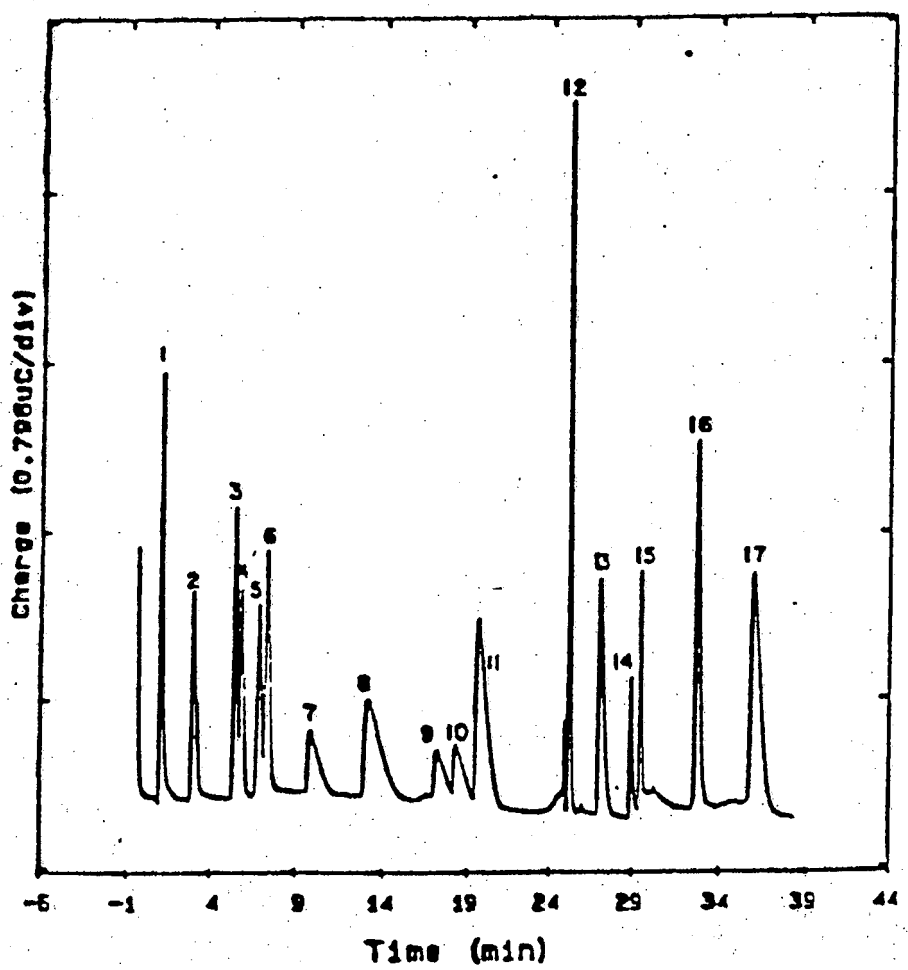
Charge (0.796uC/div)
1
2
3
4
5
6
7
8
9
10
11
12
13
14
15
16
17
-6
-1
4
9
14
19
24
29
34
39
44
Time (min)

FIG 12

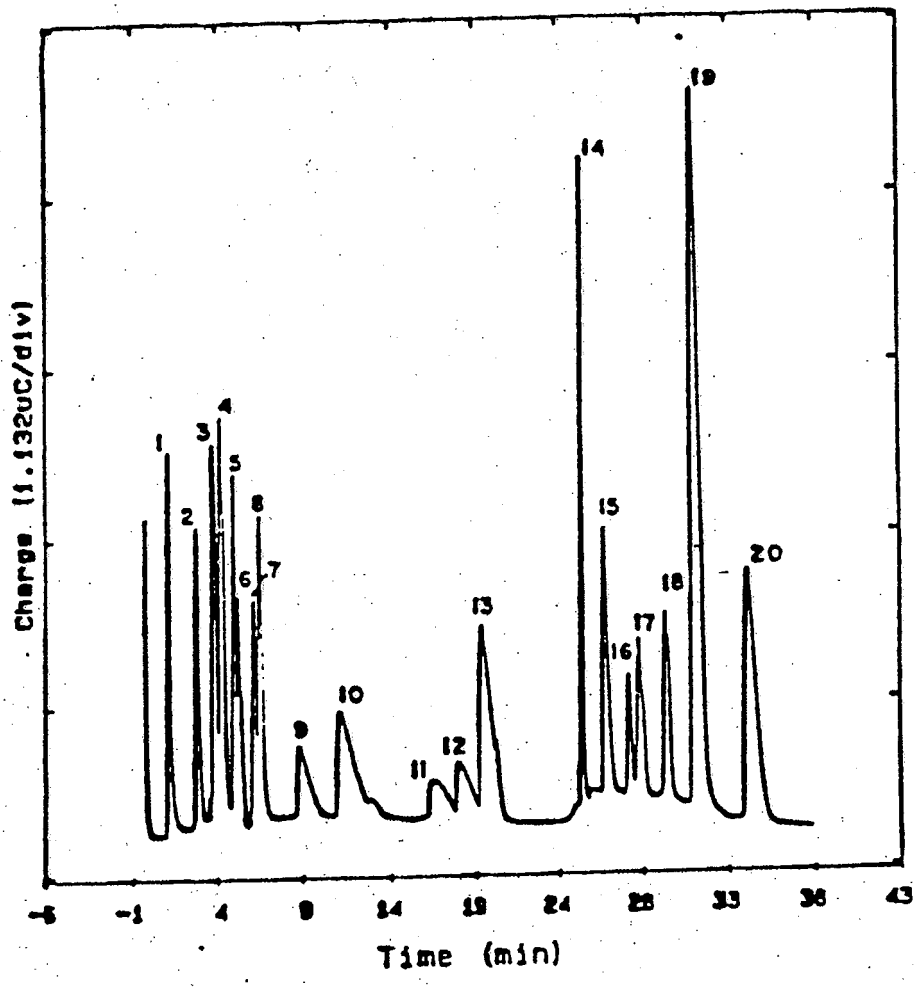
Charge (1.132uC/div)
1
2
3
4
5
6
7
8
9
10
11
12
13
14
15
16
17
18
19
20
-6
-1
4
9
14
19
24
28
33
38
43
Time (min)

FIG 13

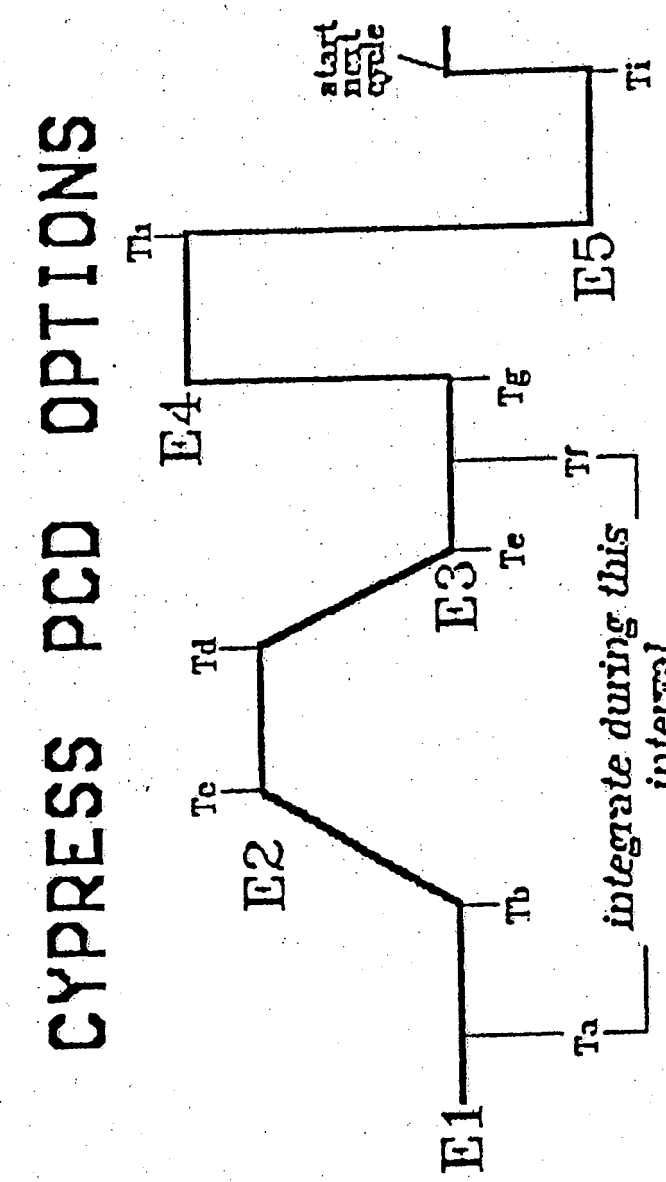
CYPRESS PCD OPTIONS
E1
E2
E3
E4
E5
Ta
Tb
Tc
Td
Te
Tf
Tg
Th
Ti
start next cycle
integrate during this interval

Fig. 14